Variable stoichiometry among core ribosomal proteins

Nikolai Slavov[a,‡], Stefan Semrau[b], Edoardo Airoldi[a], Bogdan A. Budnik[a], Alexander van Oudenaarden[b]

[a]Department of Statistics and FAS Center for Systems Biology,
Harvard University, Cambridge, MA 02138, USA
[b]Hubrecht Institute, Royal Netherlands Academy of Arts and Sciences and
University Medical Center Utrecht, Uppsalalaan 8, 3584 CT, Utrecht, The Netherlands

[‡]To whom correspondence should be addressed: nslavov@alum.mit.edu

Understanding the regulation and structure of the eukaryotic ribosome is essential to understanding protein synthesis and its deregulation in disease. While ribosomes are believed to have a fixed stoichiometry among their core ribosomal proteins (RPs), some experiments suggest a more variable composition. Reconciling these views requires direct and precise quantification of RPs. We used mass-spectrometry to directly quantify RPs across monosomes and polysomes of budding yeast and mouse embryonic stem cells (ESC). Our data show that the stoichiometry among core RPs in wild-type yeast cells and ESC depends both on the growth conditions and on the number of ribosomes bound per mRNA. Furthermore, we find that the fitness of cells with a deleted RP-gene is inversely proportional to the enrichment of the corresponding RP in polysomes. Together, our findings support the existence of ribosomes with distinct protein composition and physiological function.

Introduction

In eukaryotes, the most–studied molecular mechanisms for regulating protein translation are mediated by eukaryotic initiation factors that activate mRNAs for translation by the ribosomes and can be modulated by microRNAs and RNA binding proteins (1–5). Eukaryotic ribosomes are believed to have a fixed composition of 4 ribosomal RNAs and 80 core RPs (5–8), some of which are represented by several paralogous RPs. However, studies of eukaryotic ribosomes (9–16) have demonstrated that (i) genetic perturbations to the core RPs specifically affect the translation of some mRNAs and not others and (ii) mRNAs coding for core RPs are transcribed, spliced, and translated differentially across physiological conditions (17–23). These results suggest the hypothesis (24–26) that, depending on the tissue type and the physiological conditions, cells can alter the stoichiometry among the core RPs comprising the ribosomes and thus in

turn alter the translational efficiency of distinct mRNAs. However, differential RP–expression can reflect extra ribosomal functions of the RPs (9, 27, 28). Furthermore, polysomes (multiple ribosomes per mRNA) from different cell–lines have similar core RP stoichiometries (29). Thus, the variable RP–stoichiometry in the ribosomes of wild-type cells that is suggested by the ribosome specialization hypothesis remains unproven.

Results

Variable stoichiometry among core RPs in yeast

To measure whether the stoichiometry among RPs can change with growth conditions, we used velocity-sedimentation in $10-50\%$ sucrose-gradients to isolate fractions containing monosomes and polysomes from yeast cells grown in minimal media with either glucose or ethanol as the sole source of carbon and energy (23); see SI Appendix. Consistent with previous observations that the type and the concentration of the carbon source influence the ratio among monosomes and polysomes (30, 31), the ratio between monosomes and polysomes in our yeast cells grown in $0.4\,\%$ ethanol (Fig. 1A) or in $0.2\,\%$ glucose (Fig. 1B) is higher than is typically observed for yeast grown in rich media containing $2\,\%$ glucose. The proteins from individual fractions were spiked-in with known amounts of universal proteomics standard (UPS2) proteins, digested to peptides, labeled with tandem mass tags (TMT), and quantified on Orbitrap Elite based on the MS2 intensities of the TMT reporter ions (23); see SI Appendix for details and biological replicas. The accuracy of estimated fold-changes for peptides can be gauged by the good agreement between the measured and the spiked-in fold-changes for UPS2 (Fig. 1C) that were measured simultaneously with the yeast RPs. The measured fold–changes for UPS2 peptides are about 12% smaller than expected from the spiked-in levels, as indicated by the 0.88 slope of the linear fit in Fig. 1C, most likely due to coisolation interference (23, 32).

To quantify RP paralogs independently from one another, the fold-change of each RP was estimated as the median fold-change of its unique peptides, i.e., peptides whose sequences are found only in that RP. Our data have multiple high–confidence unique peptides for most RPs (Fig. S1A, B) except for highly homologous paralogs. These quantified unique peptides allow reproducible estimates (Fig. 1D and Fig. S1) of the relative RP levels in monosomes and polysomes collected from yeast grown in glucose or ethanol media (Fig. 1E). We systematically tested whether the variability in the estimated RP levels (Fig. 1E) reflects stoichiometry differences among the RPs or other factors and artifacts, such as noise in the MS measurements, a differential distribution of nascent RP polypeptides among monosomes and polysomes, post-translational modifications (PTMs) of the RPs, and the presence of 90S ribosomal biogenesis particles (33). These factors are unlikely to contribute significantly to the data in Fig. 1E since the majority of RP fold-changes that are estimated from multiple unique peptides differ by 10–20 % or less (Fig. S1C, D), RP fold-changes measured in independent biological replicas are highly consistent (Fig. 1D, E; $\rho = 0.96$), and the 90S particles are over 100–fold less abundant than the mature ribosomes (Fig. S2); see SI Appendix.

We find that the relative RP levels depend on two factors: the carbon source in the growth media and the number of ribosomes per mRNA (Fig. 1E). The RP levels that are higher in glucose compared to ethanol also tend to increase with the number of ribosomes per mRNA (Fig. 1E). Importantly, the RP composition of trisomes in ethanol is more similar to the composition of monosomes than to tetrasomes. This observation shows that polysomes may have similar RP composition to monosomes, suggesting that the RP composition of monosomes is not necessarily indicative of a non–functional state.

Some of the RPs without paralogs (e.g., Rpl5, Rps12, and Rps2) are enriched in monosomes and ethanol carbon source while others (e.g., Rpl39, and Rps13) are enriched in polysomes and glucose carbon source (Fig. 1E). Thus, exchange among paralogous RPs is not the sole reason for the variable RP–stoichiometry. Furthermore, while the levels of some paralogs, such as

Rpl37a and Rpl37b, are anticorrelated and consistent with paralog–exchange, the levels of other paralogs, such as Rpl17a and Rpl17b, are positively correlated and inconsistent with paralog–exchange across the analyzed ribosomes (Fig. 1E).

Variable stoichiometry among core RPs in mouse ESCs

Having found variability in the stoichiometry among yeast RPs, we sought to test its generality. We separated the ribosomes of exponentially growing mouse ESC on sucrose gradients (Fig. 2A). The ratio between the polysomal peaks and the monosomal peak is higher than the corresponding ratio in the neural tube and somites of mouse embryos (12) but lower than in many cell-lines, consistent with previous observations in mouse ESC (34). We quantified the core RPs, as annotated by Swiss–Prot, across different fractions corresponding to different numbers of ribosomes per mRNA. To control for protease–biases and to estimate the measurement noise, the proteins from each analyzed sucrose fraction were digested either with Trypsin (T) or Lys–C (L), and the data from these separate quantifications were juxtaposed in adjacent columns (Fig. 2B). As in yeast, we observe significant variation in the stoichiometry among the mouse RPs depending on the number of ribosomes bound per mRNA. For many RPs, this variability is clearly present in all replicas for both Lys-C and Trypsin digested samples; for other RPs, the variability is comparable to the noise of the measurement and thus does not correspond to biological variability. We further tested the RP variability with an independent method, Western blots. Consistently with the MS data (Fig. 2B), the Western Blots data (Fig. 2C) indicate that Rps29 and Rps14 are enriched in polysomes, Rpl11 is enriched in monosomes, and Rpl32 does not change beyond the measurement noise (loading control). Interestingly, the ratios between the polysomal and monosomal levels of mouse RPs correlate to the corresponding ratios for their yeast orthologs (Fig. 2D; p-value < 0.03), suggesting that the RP-stoichiometry differences between monosomes and polysomes are conserved across yeast and mouse.

Most variable RPs, such as Rps4x, Rps14, Rps20, Rpl5, Rpl10, and Rpl27, directly bind mRNAs (35, 36), and this binding might mediate translational regulation as previously suggested (24, 37). Furthermore, deletions or overexpressions of many of the variable RPs (Fig. 2B) have well characterized phenotypes both in development and in cancer. For example, knocking down of the polysomally enriched Rps19 (Fig. 2B) causes Diamond Blackfan anemia by selectively affecting the synthesis of some proteins but not of others (14). Interestingly, our data indicate that RPs that are frequently mutated in cancers, such as Rpl5 and Rpl10 (38, 39), are enriched in the monosomes (Fig. 2B). Conversely, RPs whose (over)–expression promotes cancer, such as Rpl30, Rps20, and Rpl39 (40, 41), are enriched in the polysomes (Fig. 2B). One interpretation, among others, of these data is that loss of function of monosomally–enriched RPs or overexpression of polysomally–enriched RPs might promote protein synthesis and cancer cell growth.

RP variability correlates to fitness

Next, we tested the variability among RPs and its phenotypic consequences by independent fitness measurements. Our observation that the RP stoichiometry depends on the number of ribosomes bound per mRNA parallels measurements of higher translational activity of polysomes compared to monosomes (42–45); some studies have even reported that the translational activity per ribosome increases with the number of ribosomes bound per mRNA (44, 45) but this finding has not been widely reproduced. We therefore hypothesized that genetic deletions of RPs enriched in the more active ribosomes – as compared to RPs enriched in less active ribosomes – may result in a larger decrease of the translation rate and thus lower fitness. To test this hypothesis, we computed the correlation (Fig. 3A) between the fitness of yeast strains with single RP–gene deletions (46) and the corresponding relative RP levels measured in the tetra-ribosomal fraction (4 ribosomes per mRNA). Consistent with our hypothesis, the fitness

of strains lacking RP–genes is inversely proportional to the relative levels of the corresponding RPs in the tetra-ribosomes (Fig. 3A). Extending this correlation analysis to the RP–levels in all sucrose fractions shown in Fig. 1E results in a correlation pattern (Fig. 3B) that further supports our hypothesis by showing the opposite dependence for fractions with fewer ribosomes per mRNA: the fitness of strains lacking RP–genes is proportional to the relative levels of the corresponding RPs in fractions with fewer ribosomes per mRNA (Fig. 3B). This correlation pattern holds both for ethanol and for glucose carbon sources. The difference in the growth media of the fitness experiments and in our experiments likely reduces the magnitude of the correlations but it is unlikely to result in observing artifactulaly significant correlations. To mitigate possible artifacts in the fitness data due to potential chromosome duplications in the deletion strains, we computed the correlations between the RP–levels and the fitness of the corresponding RP–deletion strains only for RPs without paralogs (thus unlikely to be affected by chromosome duplication) and found much higher magnitudes of the correlations (Fig. 3A, B). This result suggests that the variability in the RP stoichiometry is not limited to paralogous RPs substituting for each other.

To further test the hypothesis that the RP composition of ribosomes affects their translational activity, we used independent measurements of RP transcript levels across different growth–rates (19, 21); we examined whether differences in the growth-rate dependent transcription of RP genes are consistent with the possibility that polysome–enriched RPs are preferentially induced at higher growth–rates. For this analysis, we used the transcriptional growth-rate response that we previously quantified by growth-rate slopes that were computed by regressing RP–transcript levels on the growth-rates; all data were collected from steady–state yeast cultures grown in minimal media (19, 21). While most RP transcripts have positive growth–rate slopes, the magnitudes of these slopes (and thus the extent of growth–rate transcriptional induction) differ significantly, and some RP transcripts even have negative slopes, i.e., decrease with growth–rate (19, 21). Analogously to our fitness analysis (Fig. 3A), we correlated these growth-

rate slopes to the relative RP levels from Fig. 1E. Consistent with our hypothesis, the correlation pattern (Fig. 3C) indicates that the higher the growth–rate slope of a RP, the higher its enrichment in sucrose-fractions corresponding to increasing numbers of ribosomes per mRNA and to glucose carbon source.

We extended our fitness analysis from yeast to mouse using the published depletion data from CRISPR knockouts in human ESC (47); see SI Appendix. We used BLAST to identify the closest mouse orthologs of each human RP with deletion data (Fig. 3D), and correlated the fitness of human ESC lacking the human RP orthologs to the RP levels across sucrose fractions that we measured (Fig. 2B). The correlation pattern (Fig. 3E) is similar to the one in yeast (Fig. 3A-C) and highly significant, false discovery rate (FDR) $< 0.1\%$. This pattern indicates that the fitness of ESC lacking RP-genes is directly proportional to the relative RP levels in monosomes and inversely proportional to the relative RP levels in polysomes. The magnitude of this inverse proportionality increases with the number of ribosomes per mRNA (Fig. 3E), consistent with our hypothesis. The fact that the fitness of human ESC lacking RPs correlates significantly to the levels of the corresponding mouse orthologous RPs suggests that the variability of the RP stoichiometry and its biological function are likely conserved across mouse and human. The magnitude of this correlation increases when the correlation is computed based only on orthologs whose sequences are over 80% identical between mouse and human (Fig. 3E), providing further evidence for the conserved fitness consequences of the altered RP stoichiometry.

Discussion

A simple mechanism that may account for our observations is that the rates of translation initiation and elongation depend on the RP composition. Ribosomes whose RP composition corresponds to higher ratios between the initiation and the elongation rates are likely to be found

in fractions with multiple ribosomes per mRNA. Conversely, ribosomes whose RP composition corresponds to lower ratios between the initiation and the elongation rates are likely to be found in fractions with fewer ribosomes per mRNA. The correlations between RP–composition and fitness can be explained by the expectation that the higher the translational activity of a ribosome, the higher the fitness cost of its perturbation in rapidly growing stem cells. The key factor required for this expectation is the variable ribosomal composition that we measured. The variable RP stoichiometry in the absence of external perturbations suggests that cells use variable RP composition of their ribosomes as a regulatory mechanism of protein translation. One such example might be the preferential transcriptional induction of polysome-enriched RPs at higher growth rates (Fig. 3C).

For decades, the ribosome has been considered the preeminent example of a large RNA–protein complex with a fixed stoichiometry among the constituent core RPs (5–8). However, the direct and precise measurements of RP–levels required to support this view have been very challenging. Prior to our work, the most direct and precise quantification of RP stoichiometry that we know of is based on measuring the radioactivity from RPs labeled with ^{14}C or ^{3}H and separated on 2D–gels. Some of these studies (48, 49) achieved very high precision (standard error $< 10\ \%$) and reported over 2–fold deviation from $1:1$ stoichiometry for multiple RPs. Other studies of prokaryotic ribosomes (50) achieved lower precision, and the deviation from $1:1$ stoichiometry was within the experimental error of the measurements. The results reported in ref. (48–50) are all consistent with our findings, albeit our measurements are limited to eukaryotic ribosomes. This prior work and our measurements reflect population–averages across a heterogeneous pool of ribosomes and thus likely underestimate the magnitude of the variability among RP stoichiometries.

Our data show that the stoichiometry among RPs varies across ribosomes from different sucrose fractions. However, velocity sedimentation in sucrose gradients is unlikely to perfectly separate ribosomes based on their RP composition. For example, short mRNAs and the ribo-

somes translating them can be found only in the fractions containing few ribosomes per mRNA regardless of the efficiency of translation and the RP-composition of the ribosomes (51). Similarly, even the most highly translated mRNA that is likely to be translated by polysome-type ribosomes will go through a stage when only a single ribosome is loaded and thus will be found in the monosomal fraction. Other factors may also contribute to the mixing of different ribosomes in each sucrose fraction, including variation in the mRNA length, any degree of ribosome run-off, and mRNA shearing during sample handling, if any. None of these factors, however, can artifactually contribute to the variable RP stoichiometry that we observe. Rather, the presence of ribosomes with different RP compositions in the same sucrose fraction would average out and decrease the differences, resulting in underestimation of the RP variability.

Materials and Methods

All yeast experiments used a prototrophic diploid strain (DBY12007) with a S288c background and wild type HAP1 alleles (52). We grew our cultures in a bioreactor (LAMBDA Laboratory Instruments) using minimal media with the composition of yeast nitrogen base (YNB) and supplemented with $2g/L$ D-glucose. Before inoculation, the reactor was filled with 2L of minimal media and warmed up to a working temperature of 30^oC.

Mouse embryonic stem cells (E14 10^{th} passage) were grown as adherent cultures in 10 cm plates with 10 ml DMEM/F12 media supplemented with 10 % knockout serum replacement, nonessential amino acids (NEAA supplement), 0.1 mM β–mercapto–ethanol, 1 % penicillin and streptomycin, leukemia inhibitory factor (LIF; 1,000 U LIF/ml), and $2i$ (GSK3β and Mek 1/2 inhibitors).

Both yeast and mouse embryonic stem cells were lysed by vortexing for 10 min with glass beads in cold PLB (20 mM HEPES–KOH at pH 7.4, 1 % Triton X–100, 2 mM Magnesium Acetate, 100 mM Potassium Acetate, 0.1 mg/ml cycloheximide, and 3 mM DTT). The crude

extracts obtained from this lysis procedure were clarified by centrifugation. The resulting supernatants were applied to linear 11 ml sucrose gradients ($10\ \% - 50\ \%$) and spun at 35,000 rpm in a Beckman SW41 rotor either for 3 hours (for yeast samples) or for 2.5 hours (for mouse samples). Twelve fractions from each sample were collected using a Gradient Station. More details are available in the SI Appendix.

All data will be made available at: http://alum.mit.edu/www/nslavov/data_webs.htm

Acknowledgments

We thank J. Cate and N. Lintner for helping us colorcode the variability of RPs on the 3D structure of the yeast ribosomes, P. Vaidyanathan for help with the sucrose gradients, R. Robertson for technical assistance, and S. Kryazhimskiy, W. Gilbert, P. Vaidyanathan, G. Frenkel, D. Mooijman, D. Botstein, and A. Murray for discussions and constructive comments. This work was funded by a grant from the National Institutes of Health to A.v.O. (R01-GM068957) and Alfred P Sloan Research Fellowship to E.M.A.

References

[1] Gingras AC, Raught B, Sonenberg N (1999) eIF4 initiation factors: effectors of mrna recruitment to ribosomes and regulators of translation. *Annual review of biochemistry* 68:913–963.

[2] Hendrickson DG, et al. (2009) Concordant regulation of translation and mrna abundance for hundreds of targets of a human microrna. *PLoS biology* 7:e1000238.

[3] Sonenberg N, Hinnebusch AG (2009) Regulation of translation initiation in eukaryotes: mechanisms and biological targets. *Cell* 136:731–745.

[4] Fabian MR, Sonenberg N (2012) The mechanics of mirna-mediated gene silencing: a look under the hood of mirisc. *Nature structural & molecular biology* 19:586–593.

[5] Stillman B (2001) The ribosome. *Cold Spring Harbor Symposia on Quantitative Biology* 66.

[6] Warner JR (1999) The economics of ribosome biosynthesis in yeast. *Trends in biochemical sciences* 24:437–440.

[7] Ben-Shem A, Jenner L, Yusupova G, Yusupov M (2010) Crystal structure of the eukaryotic ribosome. *Science* 330:1203–1209.

[8] Ben-Shem A, et al. (2011) The structure of the eukaryotic ribosome at 3.0 Å resolution. *Science* 334:1524–1529.

[9] Mazumder B, et al. (2003) Regulated release of L13a from the 60S ribosomal subunit as a mechanism of transcript-specific translational control. *Cell* 115:187–198.

[10] Galkin O, et al. (2007) Roles of the negatively charged n-terminal extension of saccharomyces cerevisiae ribosomal protein s5 revealed by characterization of a yeast strain containing human ribosomal protein s5. *Rna* 13:2116–2128.

[11] Komili S, Farny NG, Roth FP, Silver PA (2007) Functional specificity among ribosomal proteins regulates gene expression. *Cell* 131:557–571.

[12] Kondrashov N, et al. (2011) Ribosome-mediated specificity in Hox mRNA translation and vertebrate tissue patterning. *Cell* 145:383–397.

[13] Topisirovic I, Sonenberg N (2011) Translational control by the eukaryotic ribosome. *Cell* 145:333–334.

[14] Horos R, et al. (2012) Ribosomal deficiencies in Diamond–Blackfan anemia impair translation of transcripts essential for differentiation of murine and human erythroblasts. *Blood* 119:262–272.

[15] Lee ASY, Burdeinick-Kerr R, Whelan SP (2013) A ribosome-specialized translation initiation pathway is required for cap-dependent translation of vesicular stomatitis virus mRNAs. *Proceedings of the National Academy of Sciences* 110:324–329.

[16] Tiruneh BS, Kim BH, Gallie DR, Roy B, von Arnim AG (2013) The global translation profile in a ribosomal protein mutant resembles that of an eIF3 mutant. *BMC biology* 11:123.

[17] Ramagopal S, Ennis HL (1981) Regulation of synthesis of cell-specific ribosomal proteins during differentiation of *Dictyostelium discoideum*. *Proceedings of the National Academy of Sciences* 78:3083–3087.

[18] Ramagopal S (1990) Induction of cell-specific ribosomal proteins in aggregation competent nonmorphogenetic *Dictyostelium discoideum*. *Biochemistry and Cell Biology* 68:1281–1287.

[19] Brauer MJ, et al. (2008) Coordination of growth rate, cell cycle, stress response, and metabolic activity in yeast. *Mol. Biol. Cell* 19:352–367.

[20] Parenteau J, et al. (2011) Introns within ribosomal protein genes regulate the production and function of yeast ribosomes. *Cell* 147:320–331.

[21] Slavov N, Botstein D (2011) Coupling among growth rate response, metabolic cycle, and cell division cycle in yeast. *Molecular Biology of the Cell* 22:1997–2009.

[22] O'Leary MN, et al. (2013) Tthe ribosomal protein Rpl22 controls ribosome composition by directly repressing expression of its own paralog, Rpl22l1. *PLoS genetics* 9:e1003708.

[23] Slavov N, Budnik B, Schwab D, Airoldi E, van Oudenaarden A (2014) Constant Growth Rate Can Be Supported by Decreasing Energy Flux and Increasing Aerobic Glycolysis. *Cell Reports* 7:705 – 714.

[24] Mauro VP, Edelman GM (2002) The ribosome filter hypothesis. *Proceedings of the National Academy of Sciences* 99:12031–12036.

[25] Gilbert WV (2011) Functional specialization of ribosomes? *Trends in biochemical sciences* 36:127–132.

[26] Xue S, Barna M (2012) Specialized ribosomes: a new frontier in gene regulation and organismal biology. *Nature Reviews Molecular Cell Biology* 13:355–369.

[27] Wool IG (1996) Extraribosomal functions of ribosomal proteins. *Trends in biochemical sciences* 21:164–165.

[28] Warner JR, McIntosh KB (2009) How common are extraribosomal functions of ribosomal proteins? *Molecular cell* 34:3–11.

[29] Reschke M, et al. (2013) Characterization and analysis of the composition and dynamics of the mammalian riboproteome. *Cell Reports* 4:1276–1287.

[30] Ashe MP, Susan K, Sachs AB (2000) Glucose depletion rapidly inhibits translation initiation in yeast. *Molecular Biology of the Cell* 11:833–848.

[31] Vaidyanathan PP, Zinshteyn B, Thompson MK, Gilbert WV (2014) Protein kinase a regulates gene-specific translational adaptation in differentiating yeast. *RNA*.

[32] Bantscheff M, Schirle M, Sweetman G, Rick J, Kuster B (2007) Quantitative mass spectrometry in proteomics: a critical review. *Analytical and bioanalytical chemistry* 389:1017–1031.

[33] Sykes MT, Shajani Z, Sperling E, Beck AH, Williamson JR (2010) Quantitative proteomic analysis of ribosome assembly and turnover *In Vivo*. *Journal of molecular biology* 403:331–345.

[34] Sampath P, et al. (2008) A hierarchical network controls protein translation during murine embryonic stem cell self-renewal and differentiation. *Cell stem cell* 2:448–460.

[35] Castello A, et al. (2012) Insights into rna biology from an atlas of mammalian mrna-binding proteins. *Cell* 149:1393–1406.

[36] Kwon SC, et al. (2013) The rna-binding protein repertoire of embryonic stem cells. *Nature structural & molecular biology*.

[37] Xue S, et al. (2015) Rna regulons in hox 5 [prime] utrs confer ribosome specificity to gene regulation. *Nature* 517:33–38.

[38] De Keersmaecker K, et al. (2013) Exome sequencing identifies mutation in cnot3 and ribosomal genes rpl5 and rpl10 in t-cell acute lymphoblastic leukemia. *Nature genetics* 45:186–190.

[39] Lawrence MS, et al. (2014) Discovery and saturation analysis of cancer genes across 21 tumour types. *Nature* 505:495–501.

[40] De Bortoli M, et al. (2006) Medulloblastoma outcome is adversely associated with overexpression of eef1d, rpl30, and rps20 on the long arm of chromosome 8. *BMC cancer* 6:223.

[41] Dave B, et al. (2014) Targeting rpl39 and mlf2 reduces tumor initiation and metastasis in breast cancer by inhibiting nitric oxide synthase signaling. *Proceedings of the National Academy of Sciences* p 201320769.

[42] Warner JR, Knopf PM, Rich A (1963) A multiple ribosomal structure in protein synthesis. *Proceedings of the National Academy of Sciences of the United States of America* 49:122.

[43] Goodman HM, Rich A (1963) Mechanism of polyribosome action during protein synthesis. *Nature* 199:318–322.

[44] Noll H, Staehelin T, Wettstein F (1963) Ribosomal aggregates engaged in protein synthesis: ergosome breakdown and messenger ribonucleic acid transport. *Nature* 198:632–638.

[45] Wettstein F, Staehelin T, Noll H (1963) Ribosomal aggregate engaged in protein synthesis: characterization of the ergosome. *Nature* 197:430–435.

[46] Qian W, Ma D, Xiao C, Wang Z, Zhang J (2012) The genomic landscape and evolutionary resolution of antagonistic pleiotropy in yeast. *Cell Reports* 2:1399–1410.

[47] Shalem O, et al. (2014) Genome-scale CRISPR-Cas9 knockout screening in human cells. *Science* 343:84–87.

[48] Weber HJ (1972) Stoichiometric measurements of 30S and 50S ribosomal proteins from *Escherichia coli*. *Molecular and General Genetics MGG* 119:233–248.

[49] Westermann P, Heumann W, Bielka H (1976) On the stoichiometry of proteins in the small ribosomal subunit of hepatoma ascites cells. *FEBS letters* 62:132–135.

[50] Hardy SJ (1975) The stoichiometry of the ribosomal proteins of *Escherichia coli*. *Molecular and General Genetics MGG* 140:253–274.

[51] Arava Y, et al. (2003) Genome-wide analysis of mrna translation profiles in saccharomyces cerevisiae. *Proceedings of the National Academy of Sciences* 100:3889–3894.

[52] Hickman M, Winston F (2007) Heme levels switch the function of Hap1 of *Saccharomyces cerevisiae* between transcriptional activator and transcriptional repressor. *Molecular and Cellular Biology* 27:7414–7424.

Figure 1. The stoichiometry among core RPs in yeast ribosomes depends both on the number of ribosomes per mRNA and on the physiological condition. Ribosomes from either ethanol (**A**) or glucose (**B**) grown yeast where separated by velocity sedimentation in sucrose gradients. The absorbance at 254 nm reflects RNA levels, mostly ribosomal RNA; see SI Appendix. The vertical dashed lines indicate the boundaries of the collected fractions. (**C**) Fold-changes estimated by MS are plotted against the fold-changes expected from the amount of universal proteomics standard (UPS2) added to sucrose fractions. All fold-changes are relative to the first data point, and the error bars are coefficients of variation. The fitted line has a slope of 0.88, indicating about 12% systematic underestimation. See SI Appendix and Fig. S1 for details and error estimates. (**D**) A comparison of biological replicas for the fold–changes of all quantified yeast RPs between the tetrasomes of yeast grown in glucose carbon source and the monosomes of yeast grown in ethanol carbon source. The ethanol samples were collected and processed independently and compared to the glucose tetrasomes; thus the noise in the scatter plot reflects all biological and technical noise in our protocols. (**E**) Levels of core RPs in the sucrose fractions estimated from their unique peptides quantified by MS. The RP levels vary depending on the carbon source (glucose or ethanol) and on the number of ribosomes bound per mRNA, indicated on the top. Monosomes from ethanol grown yeast were quantified in two biological replicas (first two columns). RP levels are plotted on a $\log_2$ scale relative to the mean levels across all fractions.

Figure 2. The stoichiometry among core RPs in mouse ribosomes depends on the number of ribosomes per mRNA. (**A**) Sucrose gradients allow separating ribosomes that are free or bound to a single mRNA (monosomes) from multiple ribosomes bound to a single mRNA (polysomes). The absorbance at 254 nm reflects RNA levels, mostly ribosomal RNA. The vertical dashed lines indicate the boundaries of the collected fractions. (**B**) The levels of core RPs in monosomes and polysomes were quantified by MS and found to vary depending on the number of ribosomes bound per mRNA. The measurement noise was estimates by (i) replica quantifications of the monosomal fraction (by using different tandem-mass-tags reporter ions, 126 or 131) and by (ii) estimating RP levels separately using either trypsin (T) or Lys–C (L) digestion, as indicated at the bottom of each column. The levels of each RP are shown on a $\log_2$ scale relative to the mean level across all fractions. See SI Appendix and Fig. S1 for more details and error estimates. (**C**) RPs were quantified by Western blots in monosomes and polysomes from high passage–number E14 mouse ESCs. Rpl32 was used as a loading control and the boxplots summarize data from 9 ratios for each quantified RP; see SI Appendix. (**D**) The $\log_2$ ratios between polysomal and monosomal levels of mouse RPs are plotted against the corresponding $\log_2$ ratios between the polysomal and monosomal levels of their orthologous yeast RPs. The significant (p-value < 0.03) positive correlation between these ratios suggests that the RP-stoichiometry differences are conserved across yeast and mouse. The plot includes all orthologous RP pairs with over 65% sequence identity between yeast and mouse.

Figure 3. The relative levels of RPs across monosomes and polysomes correlate significantly to the fitness of yeast and mammalian cells lacking the genes encoding these RPs. (**A**) The fitnesses of RP–deleted yeast strains (46) are inversely proportional (p–value $< 4 \times 10^{-3}$) to the relative levels of the corresponding RPs in tetrasomes from yeast growing on ethanol carbon source. The RPs without paralogs are marked with red squares. (**B**) Extension of the analysis in panel (A) to all sucrose fractions: correlations between the relative RP levels from Fig. 1E and the fitnesses of strains lacking the corresponding RP genes (46). The correlations are shown either for all quantified RPs or only for RPs without paralogs. (**C**) Correlations between the relative levels of the RPs from Fig. 1E and the their transcriptional growth–rate responses (slopes). The growth-rate slopes were previously computed by regressing ($R^2 > 0.87$) the levels of mRNAs in glucose-limited steady-state cultures of yeast against the growth-rates of the cultures (19, 21). (**D**) The distribution of sequence identity between human RPs and their closest mouse orthologs; the sequences and annotations for RPs are from Swiss–Prot. (**E**) Extension of the analysis for yeast in panels (A-B) to mouse: correlations between the relative levels of mouse RPs from Fig. 2B and the fitnesses of human ESC lacking the corresponding human ortholog (47). The correlations are shown either for all quantified RPs or only for RPs whose sequence identity between mouse and human exceeds $80\ \%$. All error bars are standard deviations from bootstrapping.

Figure 1

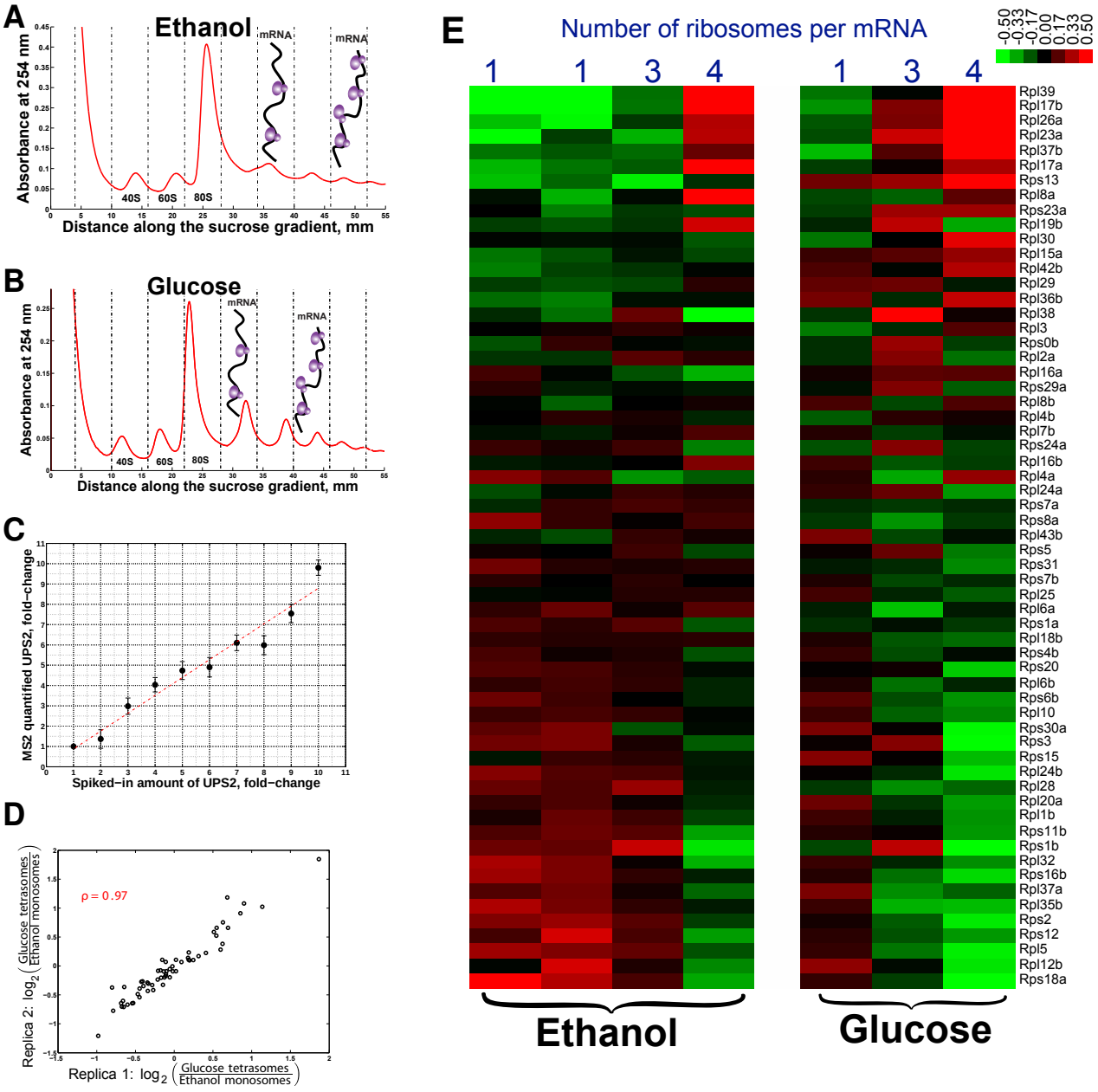

Figure 2

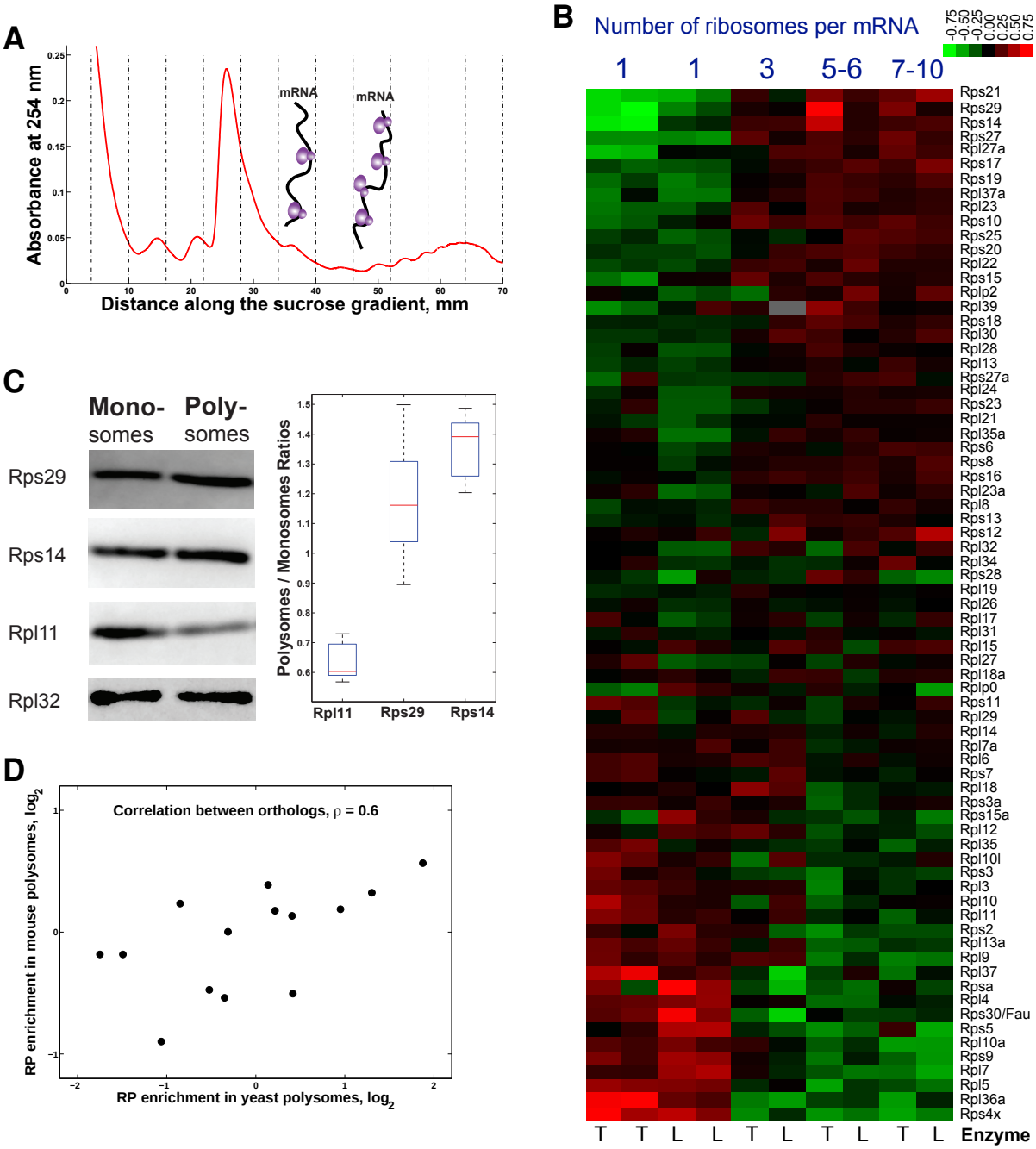

Figure 3